INTERNATIONAL JOURNAL OF MULTIDISCIPLINARY RESEARCH AND ANALYSIS

ISSN(print): 2643-9840, ISSN(online): 2643-9875

Volume 06 Issue 10 October 2023

DOI: 10.47191/ijmra/v6-i10-47, Impact Factor: 7.022

Page No. 4903-4912

Influence of Sodium Citrate Concentration on the Formation of Silver Nanoparticles and Acti Bacterials Studies

Mustafa Tareq Mahdi[1], Ali Aljalyf[2]

[1]Physics – nanotechnology / Osmania University

[2]Physics - Solid state / Mazandaran University

ABSTRACT: Silver nanoparticles (AgNPs) have been frequently studied in the scientific field due to their physical, chemical and biological properties. These characteristics are influenced by the nanomaterials' size, morphology and composition, allowing the application of AgNPs in the biomedical area due to their antimicrobial action. This work studied the influence of sodium citrate concentration on the size of silver nanoparticles. Characterization techniques such as DLS and UV-visible spectroscopy were applied to analyze nanoparticle stability, size and polydispersity index. Characterization was carried out using a UV-Vis Spectrophotometer and TEM (Transmission Electron Microscope). Analysis of the UV-Vis spectra shows that the relatively stable nanoparticles at the maximum wavelength measurement of 417 to 418 nm are synthesized using 35, 55 and 100 mmol/L of sodium citrate. Characterization using TEM and XRD analysis shows that silver nanoparticles synthesized based on sodium citrate concentration have the smallest size in the 15.5–34.56 nm range with a face-centred cubic (FCC) crystal structure. The nanoparticles utilized in this study demonstrated greater antimicrobial activity against Gram-positive bacteria than Gram-negative bacteria.

KEYWORDS: Silver nanoparticles, characterization, sodium citrate, anti-bacterial study

INTRODUCTION

Nanoscience studies materials with dimensions on the nanometer scale, that is, one billionth of a meter (10^{-9}). Nanotechnology is the study of the control and manipulation of materials to produce controllable and specific systems, with the main focus being the technological area. Nanomaterials have been attracting the attention of researchers due to their applicability in areas such as chemistry, physics and biomedicine, as on the nanometric scale, they present different properties than the macroscopic material [1]. Among nanomaterials, metallic nanoparticles stand out, as they are easy to synthesize, can be chemically modified, and have electronic and optical properties [2].

AgNPs are dynamically unstable, making it necessary to stabilize them with a stabilizing agent. This stabilization is done by electrostatic repulsion through charged species, such as cations and anions, which adsorb on the surface of the nanoparticles [3]. The use of AgNPs has been investigated in treating infections caused by bacteria or fungi, partly overlapping antibiotics due to the increasing resistance of microorganisms to these medications. Antimicrobial activity depends on the nanoparticle's diameter due to the surface area [4].

In the synthesis of nanoparticles, the reduction method is the most used, with sodium citrate ($Na_3C_6H_5O_7$) being an effective organic reducing agent that is not harmful to the environment. This molecule is widely used to reduce silver salts, enabling the formation of nanoparticles with dimensions of 30 to 100 nm and presenting an absorption band in the visible spectral range of around 420 nm, depending on the synthesis parameters [3-4]. The concentration of sodium citrate is essential in the formation of nanoparticles, as increasing the concentration of this salt provides a greater amount of reduced Ag^+ [5].

Among the characterization methods, the DLS (Dynamic Light Scattering) technique is the most common for knowing the size of nanoparticles and the polydispersity index, which can vary between 0 and 1. Values close to 0 are recorded for samples with a Uniform size distribution with a low standard deviation about the hydrodynamic diameter [6].

In this context, this work aimed to study the influence of sodium citrate concentration on the hydrodynamic size distribution of a colloidal solution of silver nanoparticles and their activity against gram positive and gram-negative bacteria's .

METHODOLOGY

All reagents were purchased from Sigma Aldrich. Firstly, the glassware was washed with aqua regia in a 1:3 ratio of nitric acid (HNO_3) and hydrochloric acid (HCl) to remove contaminating metals. The synthesis of silver nanoparticles was based on the method described in 1982 by Lee and Meisel[7]. The synthesis was started with 91.11 mg of $AgNO_3$ solubilized in 50 mL of type I water, maintaining constant stirring at 500 rpm and 90ºC. A solution prepared with 5 mL of different concentrations of sodium citrate (Sigma Aldrich) was added to this mixture, namely 35 mmol/L, 55 mmol/L, and 100 mmol/L

The system was kept under stirring and heating for 30 min, starting counting after adding sodium citrate. The colour changed, as recorded in the photos in Image 1. The synthesis was stored at room temperature in an amber bottle.

The UV-Vis spectra in the 200 to 800nm region of the suspensions containing the metallic nanoparticles were obtained on an Agilent UV-Vis diode array spectrophotometer. X-ray diffraction analyses were performed on the Shimadzu X-ray diffractometer, model XRD6000, operating with CuKα radiation (λ = 1.54 Å), voltage of 40 kV, current of 30 mA, scanning speed of 20/min and region of 2θ between 30 and 90º. Vibrational spectroscopy in the infrared region of silver nanoparticles was obtained by depositing a drop of the colloidal suspension of silver particles on a zinc selenide (ZnSe) window, and the spectrum was obtained on an FT-IR spectrophotometer Bomem MB series in the range of 4000 to 400 cm^{-1} and resolution of 4 cm-1, using 16 accumulations per spectrum. Transmission electron microscopy (TEM) images were obtained using JEOL 1230 model, operating at 80 kV. A drop of the suspension containing silver nanoparticles was deposited on a copper grid containing a thin film of carbon-stabilized palladium and dried under ambient.

Image 1: Synthesis of silver nanoparticles.

ANTIMICROBIAL ACTIVITY

This subsection will present the microbiological tests that were carried out to evaluate the antimicrobial activity of the synthesized nanoparticles.

Agar diffusion test: The agar diffusion test was carried out to qualitatively evaluate the antimicrobial potential of the synthesized nanoparticles against bacterial strains. The test was performed with two Gram-positive bacteria, *Streptococcus pneumoniae* (ATCC 33400) and *Enterococcus faecium* (ATCC 35667), and two Gram-negatives, *Escherichia coli* (ATCC 35218) and *Pseudomonas aeruginosa* (ATCC 27853). Standard strains were used because they are considered potential food pathogens.

Standard autoclave sterilization was performed to ensure the culture medium, glassware, and tips sterility. Culture media were prepared first: 1) Petri dish Müller-Hinton (MH) agar; 2) broth. At 121°C and 1 atm pressure, a vertical autoclave sterilized both media for 15 min. A platinum loop was used to inoculate bacteria into MH broth in tubes in laminar flow. One tube per inoculated bacteria. These were incubated overnight (12 h) at 35 ± 0.5ºC. Following the 0.5 McFarland scale, each tube's bacterial cell concentration was diluted sequentially until 10^5 CFU/ml. Shimadzu UV-1601PC UV-visible equipment measured 600nm turbidity. Next, 100 µL of diluted samples were spread on MH agar using the Drigalski loop. Eight Petri dishes were used for each bacterium, seven for each synthesis and one control (no nanoparticles, only bacteria)—next, a spatula deposited nanoparticles on the plates. Three nanoparticle spots were deposited on each bacteria plate using 0.4 mg of sample. Each bacterium was treated this way. After this stage, the plates were incubated in a microorganism-friendly oven at 35 ± 0.5ºC for about 24 hours. Inhibition halos were visible after this time. Calliper measurements were made of inhibition halos' diameters.

Shake flask method [9]: In addition to the diffusion test (in a solid medium), a shaking test was carried out in a flask (in a liquid medium), followed by plating the samples and counting the bacterial colonies after 24 h (CFU/ml). For this test, the bacterial strains that showed greater inhibition in the previous test were used, that is, *Streptococcus pneumoniae* as Gram-positive and *Escherichia coli* as Gram-negative, and the syntheses that obtained smaller nanoparticles and that at the same time formed halos in more bacteria in the diffusion test. In this experiment, 3 different concentrations of AgNPs (100 mmol/L solidum citrate) were tested in addition to the control containing only the bacteria (C0). These concentrations used were 100 µg/ml (C1), 250 µg/ml (C2) and 500 µg/ml (C3), all of which were carried out in triplicates. This test was divided into 4 days. On the first day, TSB (Tryptic Soy Broth) medium was made for both the flasks where the nanoparticles were deposited for shaking on the second day and for

the tubes where the bacteria grew. Using an inoculation loop, each bacterium was picked from a stock culture into tubes containing TSB medium and incubated overnight (12 h) at 35 ± 0.5ºC. On the second day, based on the McFarland 0.5 scale (estimated at 10^8 CFU/ml), the concentration of bacterial cells was adjusted by dilutions until a final concentration of 105 CFU/ml. To read turbidity (600 nm), use the UV-Visible technique. In laminar flow, 100 µl of the adjusted bacterial suspension was deposited in each flask (already prepared on the first day with the medium), and the nanoparticles were weighed according to the mentioned concentrations. They were then placed under agitation at 165 rpm, 35ºC for 24 hours.

A PCA (Plate Count Agar) medium was prepared on the third day. Samples that were agitated were diluted in phosphate-buffered saline. For *S. pneumoniae*, the decimal dilutions of C0 plated were 10^{-7}, 10^{-8} and 10^{-9}; for C1, C2 and C3 they were 10^{-2} to 10^{-7}. For *E. coli*, the C0 dilutions were the same; for C1, C2 and C3, they were generally from 10^{-5} to 10^{-8}. Plating was performed using the pour plate technique, adding a 1 ml aliquot of the dilution to the Petri dish, pouring 35 ml of the PCA culture medium over the inoculum and homogenizing appropriately. After the medium solidified, the inverted plates were incubated at 35ºC for 24 hours. On the last day (fourth day), colonies were counted on the plates using the Manual Colony Counter Model CP 608 from Phoenix-Luferco. The count was after the incubation time, expressed in CFU/ml. It was carried out on plates that showed 30 to 300 colonies, and this value was multiplied by the inverse of the dilution.

RESULTS AND DISCUSSION

The graphs in Figure 1 show the results of the UV-visible analyses, with emphasis on the surface plasmon resonance (SPR) region.

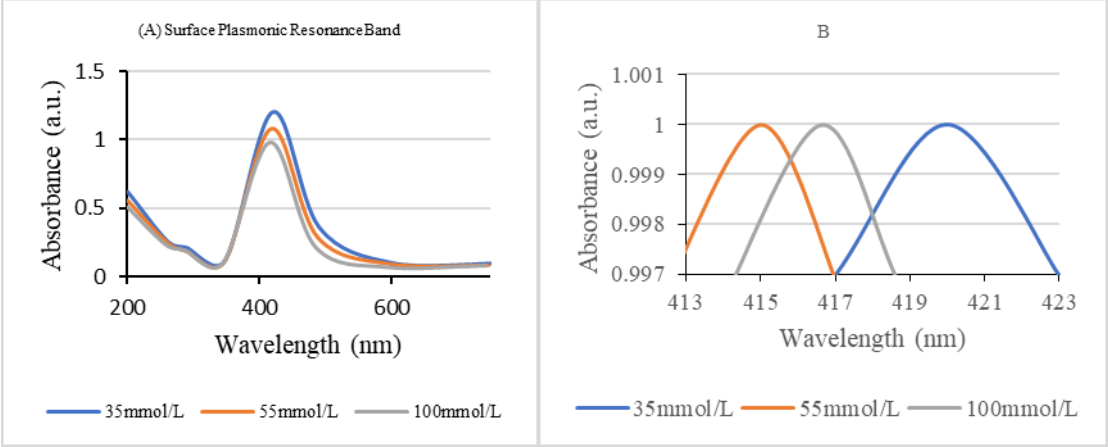

Figure 1: a) UV-visible analysis of the samples and b) magnification of the SPR region.

The graphs in Figure 2 show the results of the DLS analyses for the different concentrations of Sodium citrate. The results clearly show two populations of sizes.

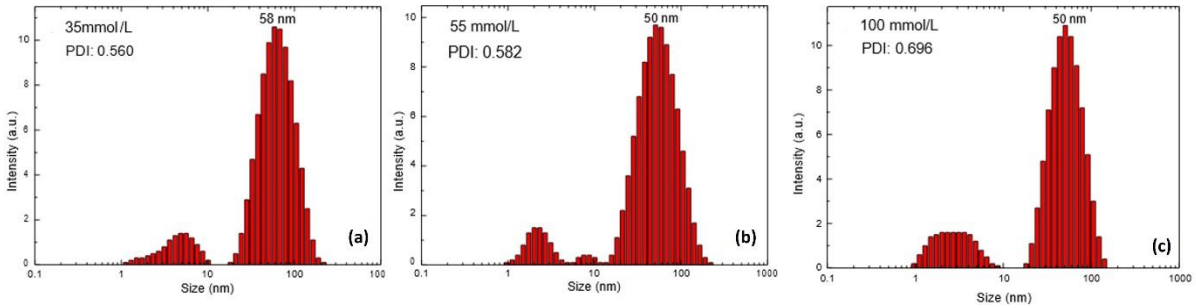

Figure 2: Graph with size distribution with sodium citrate concentrations: a) 35mmol/L; b) 55mmol/L; c) 100 mmol/L.

To evaluate the size distribution, the most intense bands in these graphs were analyzed by fitting Gaussian curves, considering that the width value at half height may suggest more uniformity of particles with larger sizes (Figure 3a). At the same time, Figure 3b allows the analysis of colloidal stability.

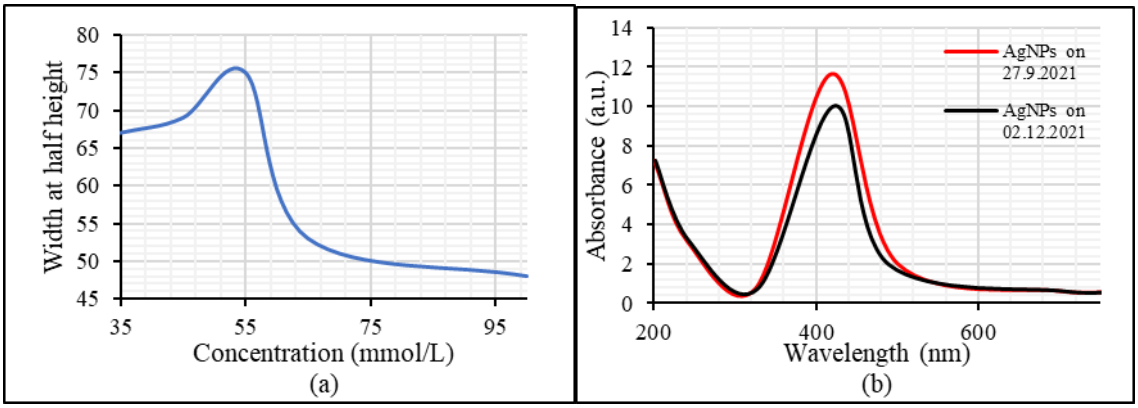

Figure 3: a) Graph of the analysis of the width at half height of the bands with greater intensity of the size distributions of colloidal syntheses b) Stability analysis

In Figure 2, the graphs present a size distribution that indicates the formation of nanoparticles with different diameters for each concentration of sodium citrate studied. Using these histograms, an average polydispersity index (PdI) value of 0.639 was obtained, indicating an average result due to the wide range of sizes in the colloidal solution. However, the value of the width at half height was calculated. Figure 3-a shows that the best sodium citrate concentration was 100 mmol/L due to a more uniform hydrodynamic diameter distribution.

Figure 3-b compares the UV-visible spectra of a single sample over a three-month interval. These data indicate good stability of the silver nanoparticles as a small shift in wavelength is observed, being 416 nm immediately after the end of the synthesis and 418 nm three months later, which may suggest good stability of the colloidal solution.

FT IR Analysis: The use of sodium citrate in the preparation of silver nanoparticles aimed to generate a complex with the precursor ($AgNO_3$) and control the growth and agglomeration of silver nanoparticles and, in this way, obtain uniform nanoparticles in size.

To investigate the chemical interaction between sodium citrate and silver nanoparticles, the infrared spectra of pure sodium citrate and synthesized nanoparticles were obtained, which are shown in Fig. 4. The infrared spectrum of pure sodium citrate presents two main bands at 1019 cm^{-1} and 1663 cm^{-1} which correspond [10], respectively, to the vibrations of the C-N and C=O bonds, with a change in these bands indicating the formation of the sodium citrate complex with silver nanoparticles. Comparing the spectra, it is possible to observe a change in the band's position from 1667 cm^{-1}, characteristic of pure sodium citrate, to 1644 cm^{-1}, the latter corresponding to sodium citrate associated with silver nanoparticles. This result suggests that an interaction occurred between the sodium citrate molecules and the surface of the silver nanoparticles, forming the Ag/sodium citrate coordination complex. When studying the stabilization mechanism of sodium citrate in the preparation of silver nanoparticles with a size smaller than 50 nm, Xu et al (2020) [11]. proposed the coordination between the nitrogen of the sodium citrate structure and the silver by infrared analysis in conjunction with electron microscopy images of streaming. However, when silver nanoparticles had sizes between 500 and 1000 nm, the coordination was attributed to interactions with both the nitrogen and oxygen of the sodium citrate molecules[12].

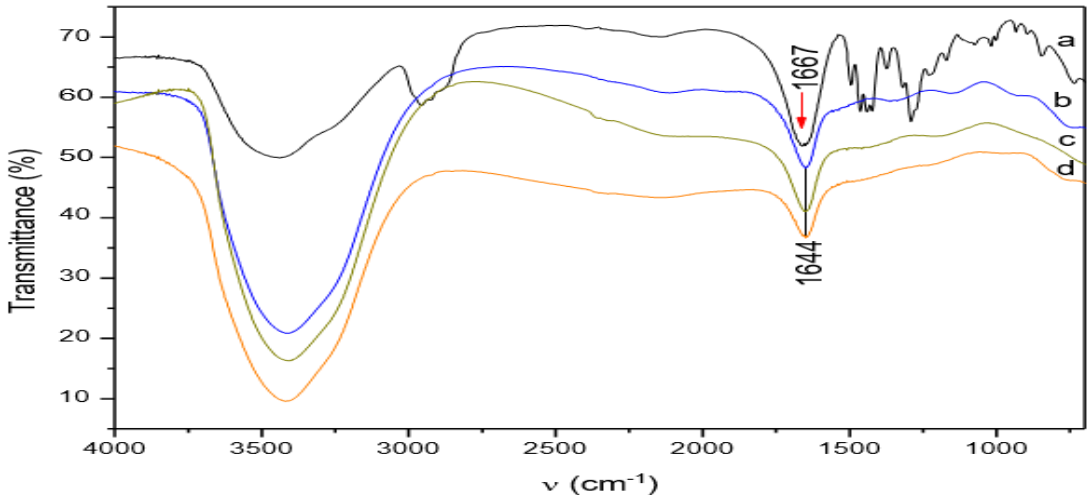

Figure 4: FTIR spectra of silver nanoparticles obtained from different concentrations of $AgNO_3$. (a) Pure sodium citrate ; b) $AgNO_3$-sodium citrate 100mmol/L ; c) $AgNO_3$-sodium citrate 55mmol/L and d) $AgNO_3$-sodium citrate 35mmol/L .

Influence of Sodium Citrate Concentration on the Formation of Silver Nanoparticles and Acti Bacterials Studies

XRD analysis: The X-ray diffraction patterns of the nanoparticles formed at different concentrations of Sodium citrate are shown in Fig.5. The peaks at 37.8°, 43.8°, 64.2°, 77.2° and 81.5° are correlated with the crystal planes (111), (200), (220), (311) and (222), typical of the face-cantered cubic structure. Lee et al. showed that the reaction between silver nitrate and sodium citrate as a stabilizer resulted in spherical nanoparticles and triangular nanoplates forming. The morphology of silver nanoparticles with a face-cantered cubic structure was found to depend on the Ag^{+}/sodium citrate ratio. Cobos et al.(2020) [13] followed the formation of silver nanoparticles by XRD from AgNO3 and sodium citrate. They observed that the particle size was influenced by the preparation temperature and concentration of the precursor.

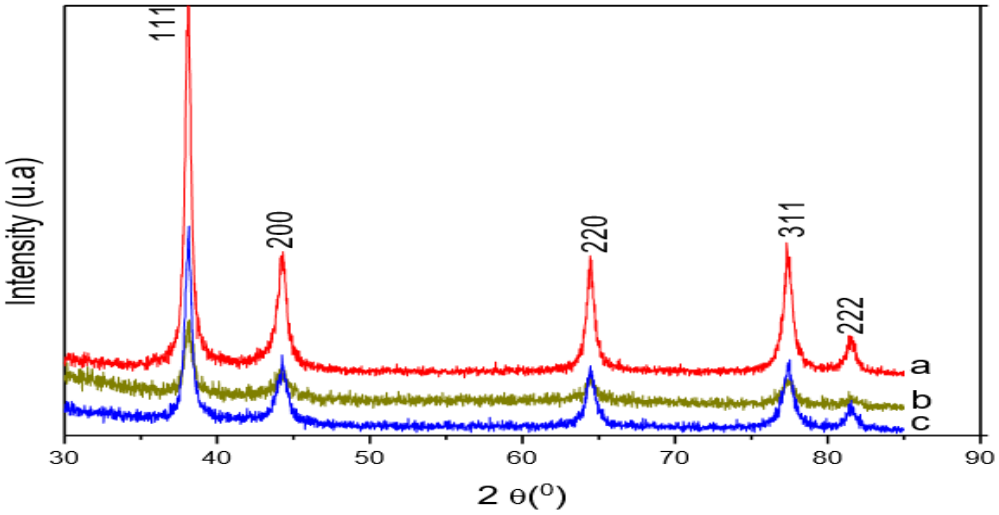

Figure 5: X-ray diffraction pattern of silver nanoparticles obtained from different concentrations of Sodium citrate: a) 35mmol/L, b) 55mmol/L, and c) 100mmol/L

Characterization of silver nanoparticles by TEM

The transmission electron microscopy technique was used to investigate the morphology, size and dispersion of silver nanoparticles. Fig.6 shows the transmission electron microscopy images obtained for the nanoparticles prepared from different precursor concentrations, using sodium citrate as a stabilizer. It was observed that the preparation conditions can control the size distribution and the coalescence of the nanoparticles. In this case, using a lower concentration of $AgNO_3$ allowed silver nanoparticles to be obtained with uniform size and good dispersion.

The formed silver nanoparticles were examined using TEM to ascertain their shape and demonstrate that they were nanoscale particles. Shape and Size Characterization of Silver Nanoparticles The results of TEM analysis shown in Figure 6 show that the morphology is less uniform, and the particle size is large but still on the nanometre scale. This is influenced by the formation of aggregates from silver nanoparticles and the presence of Ag+ ions, which have not been completely reduced. The size of the silver nanoparticles produced is 36 ± 4.96 nm.

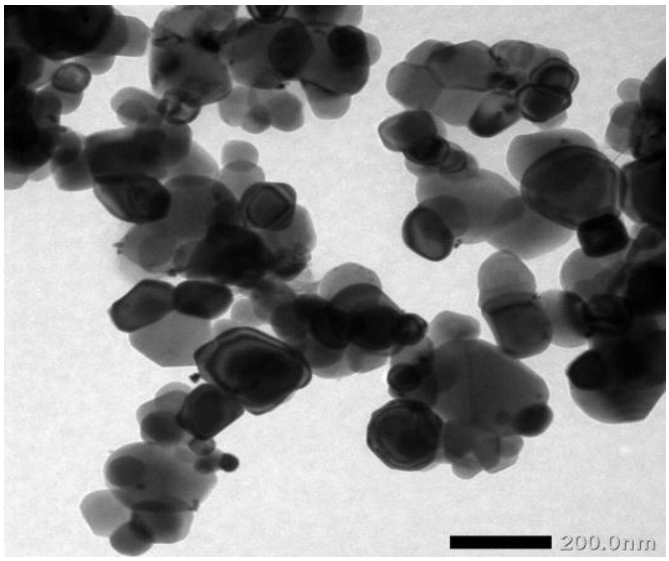

Figure 6: Shape of silver nanoparticles synthesized using $AgNO_3$ precursor and 100mmol/L sodium citrate as reductant.

Influence of Sodium Citrate Concentration on the Formation of Silver Nanoparticles and Acti Bacterials Studies

The abundance of electrons in silver (Ag) affects the size of the silver nanoparticles produced; the more stable the silver nanoparticles produced, the more homogeneous and difficult to aggregate they will be in size.

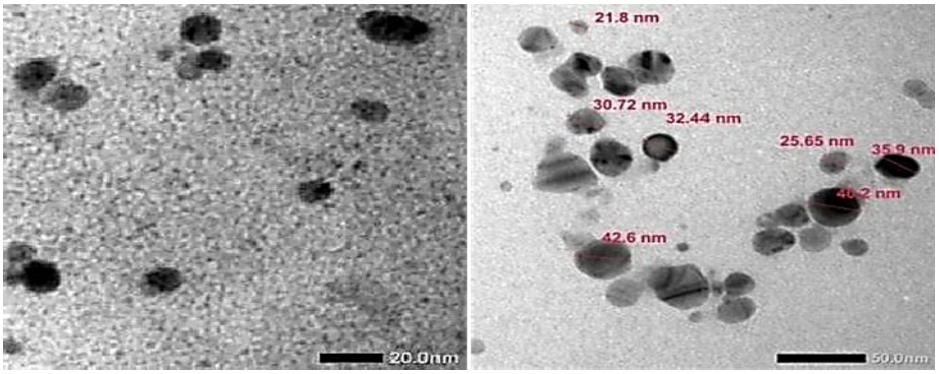

Figure 7. Results of TEM photos of synthesized silver nanoparticles sample with 35 mmol/L sodium citrate at a magnification of 150,000x (A) and 100,000x (B)

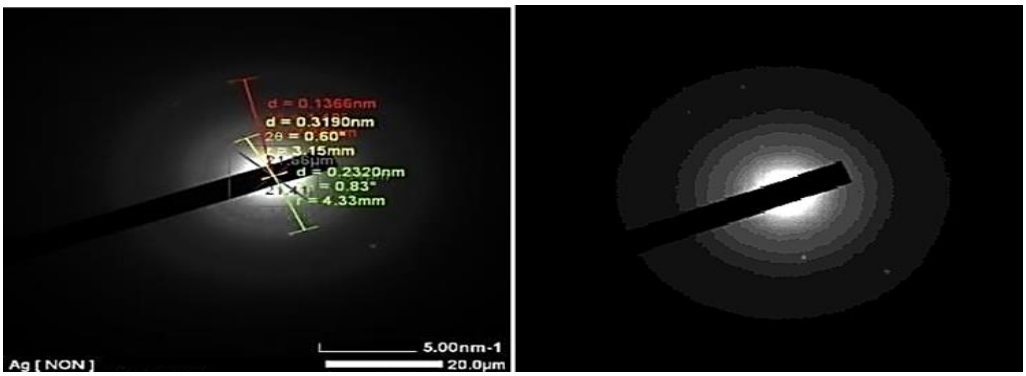

Figure 8. Diffraction pattern of silver nanoparticles sample with 35 mmol/L sodium citrate before (A) and after (B) the diffraction data was measured

Figure 9. Results of TEM photos of synthesized silver nanoparticles with 55 mmol/L sodium citrate samples at a magnification of 150,000x (A) and 100,000x (B)

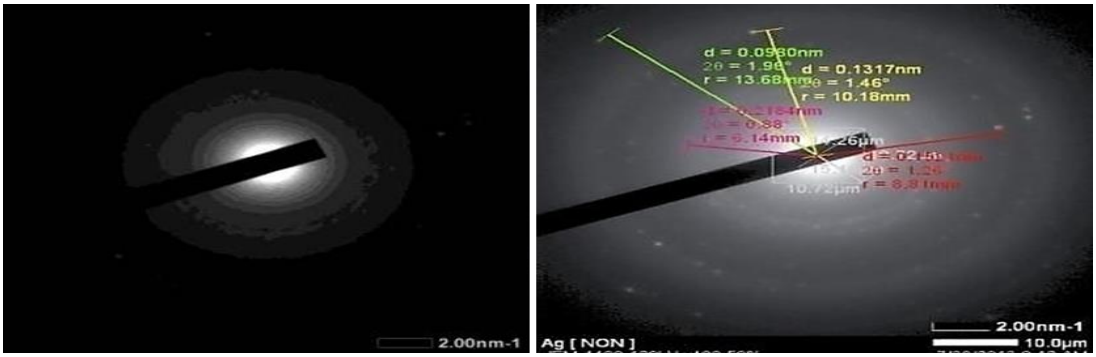

Figure 10. Diffraction pattern of silver nanoparticles sample with 55 mmol/L sodium citrate before (A) and after (B) the diffraction data was measured

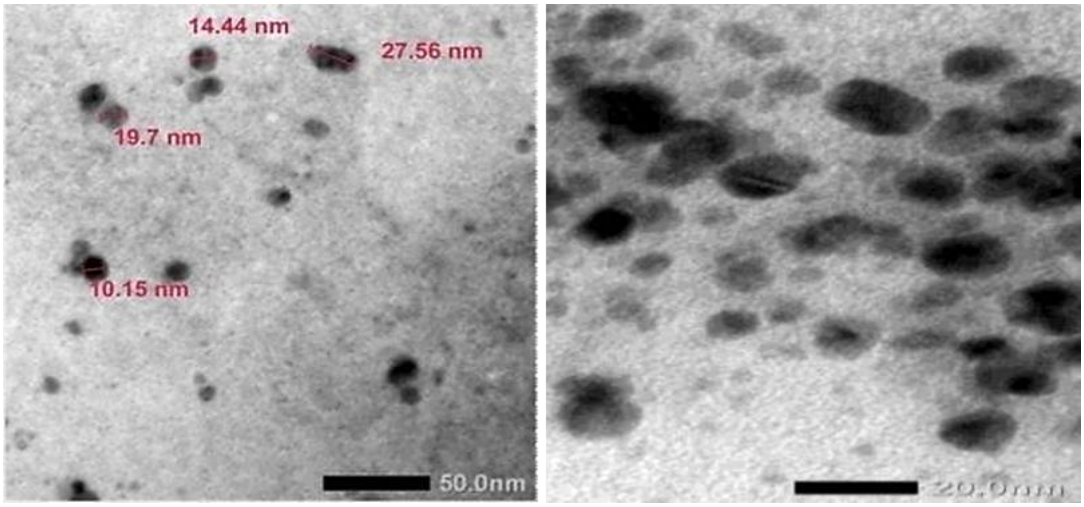

Figure 11. Results of TEM photos of synthesized silver nanoparticles sample with 100 mmol/L sodium citrate at 150,000x (A) and 100,000x (B) magnification

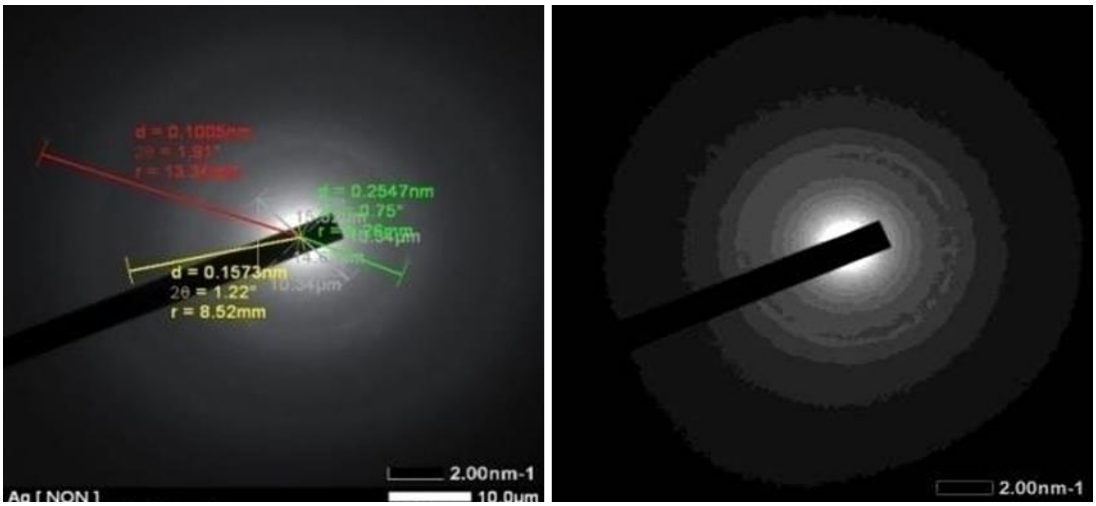

Figure 12. Diffraction pattern of silver nanoparticles sample with 100 mmol/L sodium citrate before (A) and after (B) the diffraction data was measured

Based on the results of TEM analysis (Figures 7 to 12), the sodium citrate concentration can produce the smallest silver particle size, namely 36 ± 4nm. Using 55mmol/L sodium citrate in synthesis can also inhibit the growth of silver nanoparticles and prevent accumulation so that the particles do not grow larger. Also, the 100mmol/L sodium citrate sample produced the smallest silver particle size. Therefore, sodium citrate in the same concentration, which plays a role in retaining and stabilizing small amounts of silver nanoparticles, can effectively produce silver nanoparticles that are small in size. Lee et al. (2019)[14] synthesised silver nanoparticles by varying the mole ratio of the reducing agent to $AgNO_3$ precursor, producing nanoparticles of various sizes. This shows that the synthesized colloidal nanoparticles were proven to have a morphology and particle size distribution that depended on various reaction conditions, such as the concentration of $AgNO_3$ and the mole ratio of the reducing agent to $AgNO_3$ salt.

ANTI-BACTERIAL ACTIVITY

Agar diffusion test: Figure 13 displays the outcomes of the diffusion test for silver nanoparticles. The synthesis results demonstrated that *S. pneumoniae* and *E. faecium*, two Gram-positive bacteria, formed a distinct inhibition halo. At the same time, a subtle inhibition halo can be seen forming for Gram-negative bacteria like *E. coli* and *P. aeruginosa*. The average diameters of the inhibition halos for *S. pneumoniae* are 17 mm ±0.16. For *E. coli*, it was 15 mm ±0.3, and for *P. aeruginosa*, it was 12 mm± 0.02. The *S. pneumoniae* bacterium was discovered to have a higher sensitivity. The effectiveness of silver nanoparticles, with the average size of the obtained silver nanoparticles being around 18 nm, can be attributed, in Salleh et al. (2020)[15], to the small size of the NP and consequently a larger surface area.

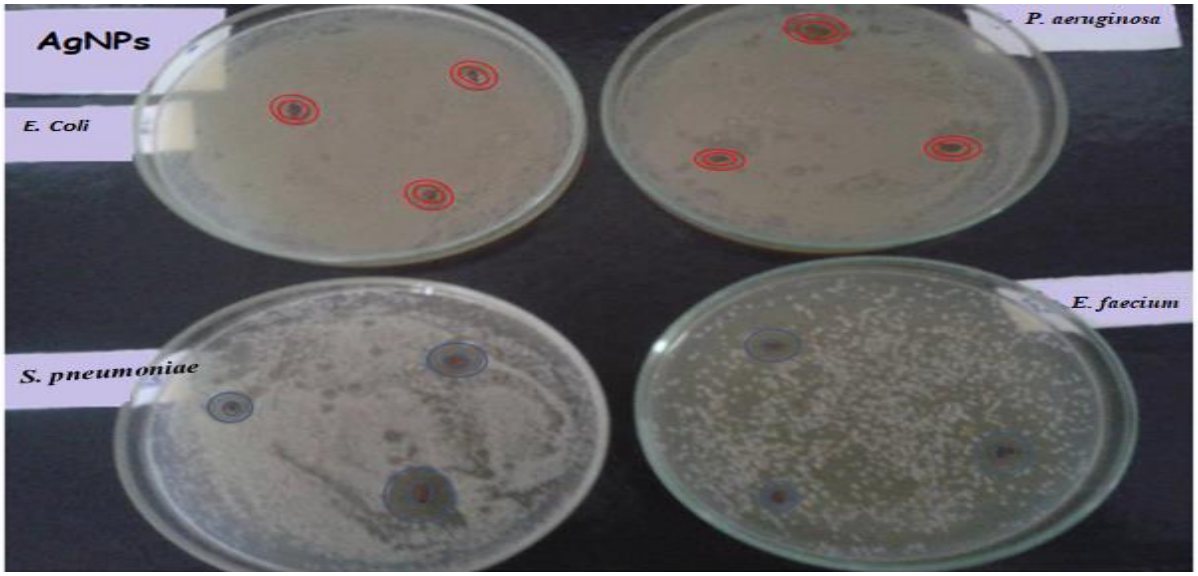

Figure 13: Inhibition halo test for the synthesis of AgNPs, showing the formation of the inhibition halo for Gram-positive bacteria (blue) and Gram-negative bacteria (red).

FLASK SHAKES TEST

The flask shaking test was carried out with the Ag nanoparticles synthesized by the precipitation method. For control (C0), colony counting was performed at dilution 10^{-8}; for C1, it was dilution 10^{-5}; for C2 and C3, at dilution 10^{-4}. In other words, there was also a gradual inhibition about the control.

The graph (Fig 14) was generated through statistical analysis of the results obtained by counting *S. pneumoniae* bacteria colonies under the action of Ag nanoparticles. Concentration C1 had a high inhibition about the control, less than 100%, while at other concentrations, C2 and C3, we already obtained an inhibition of approximately 100%. But with a concentration of around 180 µg/ml, it would be possible to obtain maximum inhibition.

The greater efficiency of silver nanoparticles is due to the greater surface area available for interactions. The penetration of the nanoparticle into the bacterial cell wall depends on its size, and this ease of penetration was also observed in other studies [16-17].

According to some studies, the primary respiratory enzymes' thiol groups could be the molecular targets of silver ions. AgNPs may also affect the phospholipid region of bacterial membranes [17-18]. Regarding *E. coli* bacteria, for the control, the counting of bacterial colonies was carried out at dilution 10^{-8}, while for concentrations C1, C2 and C3 it was at dilution 10^{-7}. In other words, a lower inhibition than the result obtained with the *S. pneumoniae* bacteria.

The graph of the statistical analysis of the results obtained with the counting of *E. coli* bacteria colonies under the action of Ag nanoparticles can be seen below (Figure 14). For C1, an inhibition of around 45% was obtained about the control; for C2, around 73% inhibition; and for C3 an inhibition of almost 90% (same pattern as for the other nanoparticles).

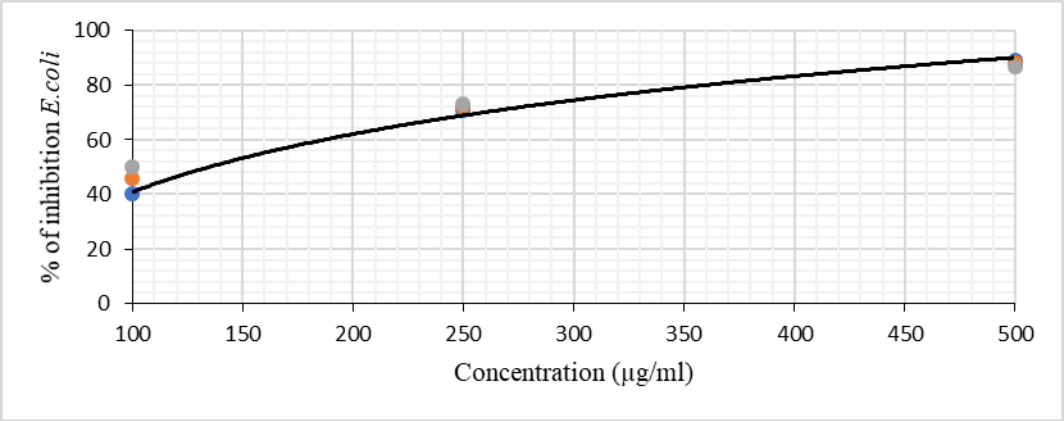

Figure 14: Graph of the percentage of inhibition of *E. coli* bacteria about the control at different concentrations of AgNPs used in the experiment.

In the work of Gouyau et al. (2021) [19], it was demonstrated that the concentration of Ag nanoparticles to inhibit bacterial growth varies according to the type of bacteria. However, all the bacteria in their study, including *E. coli*, did not show significant

growth at NP concentrations above 75 µg/ml. They also state that the antimicrobial activity of AgNPs is size-dependent; in their work, they obtained NPs around 10-20 nm.

In the work of Yuan et al (2017) [20], the evaluation of Ag nanoparticle activity showed that the bacterial growth of both *E. coli* and *S. pneumoniae* treated with 25 µg/ml of AgNPs was slightly lower than the control, while when treated with 50 and 100 µg/ml NPs, bacterial growth was greatly inhibited.

In studies by Liao et al (2019) [21], different concentrations of Ag nanoparticles were evaluated about the number of colonies formed by *E. coli* bacteria and the influence on their respective growth. The 10 µg/ml concentration inhibited 70% of bacterial growth, and a 50-60 µg/ml concentration caused 100% inhibition. In their study, silver nanoparticles were 12 mm in diameter. When *E. coli* is treated with metal oxide nanoparticles, the bacterial membrane shows a significant increase in permeability, making the cell unable to regulate transport. The outer membrane present in *E. coli* provides an effective permeability barrier. Some studies [22] on the mechanism of action of silver ions (Ag+) in bacteria report that the inhibitory effect of Ag+ is also related to the electrostatic attraction between the negatively charged cell wall and the positive charge of the ions.

CONCLUSION

In this work, it was possible to study the influence of sodium citrate on the formation of silver nanoparticles. Spectral analyses showed a variation in the absorption of the plasmonic resonance band, which indicates a greater reduction in silver. It was not possible to identify a variation in the polydispersity index (PdI), however, the results suggest that the best concentration of sodium citrate was 100 mmol/L. The nanoparticles were stable over three months, showing a low band shift in the UV-visible spectrum. The appearance of the plasmon band in the region between 410 and 420 nm of the spectrum was attributed to the formation of spherical silver nanoparticles. X-ray diffractograms revealed the formation of silver nanoparticles with a face-cantered cubic structure. FTIR analysis confirmed the formation of the Ag/sodium citrate complex based on the change in the peak position at 1667 cm-1 of pure sodium citrate to 1644 cm^{-1} relative to silver nanoparticles stabilized with sodium citrate. Transmission electron microscopy images indicated that the concentration of the precursor has an important effect on the dispersion and size distribution of the nanoparticles. At 100 mmol/L, sodium citrate nanoparticles were obtained that were more uniform in size and more dispersed. The results of bacterial tests showed that the nanoparticles used had greater antimicrobial efficacy against Gram-positive bacteria than Gram-negative bacteria. In a quantitative flask shaking test to measure the inhibitory effect of nanoparticles on *S. pneumoniae*, the tested nanoparticles they demonstrated significant bactericidal activity of approximately 100% compared to the control group. It should be noted that the control group contained a lower concentration of AgNPs. Compared to the control group, *E. coli* showed a significant reduction of approximately 90% when exposed to the three nanoparticles (NPs) with the highest concentration studied.

REFERENCES

1) Gandhi M, Amreen K. Emerging Trends in Nanomaterial-Based Biomedical Aspects. *Electrochem*. 2023; 4(3):365-388.
2) Harish V, Ansari MM, Tewari D, Gaur M, Yadav AB, García-Betancourt M-L, Abdel-Haleem FM, Bechelany M, Barhoum A. Nanoparticle and Nanostructure Synthesis and Controlled Growth Methods. *Nanomaterials*. 2022; 12(18):3226
3) Boughbina-Portolés A, Sanjuan-Navarro L, Moliner-Martínez Y, Campíns-Falcó P. Study of the Stability of Citrate Capped AgNPs in Several Environmental Water Matrices by Asymmetrical Flow Field Flow Fractionation. *Nanomaterials*. 2021; 11(4):926.
4) Sánchez-López E, Gomes D, Esteruelas G, Bonilla L, Lopez-Machado AL, Galindo R, Cano A, Espina M, Ettcheto M, Camins A, et al. Metal-Based Nanoparticles as Antimicrobial Agents: An Overview. *Nanomaterials*. 2020; 10(2):292.
5) La Spina R, Mehn D, Fumagalli F, Holland M, Reniero F, Rossi F, Gilliland D. Synthesis of Citrate-Stabilized Silver Nanoparticles Modified by Thermal and pH Preconditioned Tannic Acid. *Nanomaterials*. 2020; 10(10):2031.
6) Kim A, Ng WB, Bernt W, Cho NJ. Validation of Size Estimation of Nanoparticle Tracking Analysis on Polydisperse Macromolecule Assembly. *Sci Rep.* 2019 Feb 25;9(1):2639.
7) Lee P.C., Meisel D. Adsorption and Surface-Enhanced Raman of Dyes on Silver and Gold Sols. *J. Phys. Chem.* 1982;86:3391–3395.
8) Ingerslev F, Nyholm N. Shake-flask test for determination of biodegradation rates of (14)C-labeled chemicals at low concentrations in surface water systems. *Ecotoxicol Environ* Saf. 2000 Mar;45(3):274-83.
9) Jin H, Cai M, Deng F. Antioxidation Effect of Graphene Oxide on Silver Nanoparticles and Its Use in Antibacterial Applications. *Polymers*. 2023; 15(14):3045.

10) Giri, Anupam & Makhal, Abhinandan & Ghosh, Barnali & Raychaudhuri, Arup & Pal, Samir.Functionalization of manganite nanoparticles and their interaction with biologically relevant small ligands: Picosecond time-resolved FRET studies. *Nanoscale.* 2010: 2. 2704-9.
11) Xu L, Wang YY, Huang J, Chen CY, Wang ZX, Xie H. Silver nanoparticles: Synthesis, medical applications and biosafety. Theranostics. 2020 Jul 11;10(20):8996-9031.
12) Ranoszek-Soliwoda K, Tomaszewska E, Socha E, Krzyczmonik P, Ignaczak A, Orlowski P, Krzyzowska M, Celichowski G, Grobelny J. The role of tannic acid and sodium citrate in the synthesis of silver nanoparticles. *J Nanopart Res.* 2017;19(8):273.
13) Cobos M, De-La-Pinta I, Quindós G, Fernández MJ, Fernández MD. Graphene Oxide–Silver Nanoparticle Nanohybrids: Synthesis, Characterization, and Antimicrobial Properties. *Nanomaterials*. 2020; 10(2):376
14) Lee SH, Jun B-H. Silver Nanoparticles: Synthesis and Application for Nanomedicine. *International Journal of Molecular Sciences*. 2019; 20(4):865.
15) Salleh A, Naomi R, Utami ND, Mohammad AW, Mahmoudi E, Mustafa N, Fauzi MB. The Potential of Silver Nanoparticles for Antiviral and Antibacterial Applications: A Mechanism of Action. *Nanomaterials*. 2020; 10(8):1566.
16) Bruna T, Maldonado-Bravo F, Jara P, Caro N. Silver Nanoparticles and Their Antibacterial Applications. *Int J Mol Sci*. 2021 Jul 4;22(13):7202.
17) Zhang XF, Liu ZG, Shen W, Gurunathan S. Silver Nanoparticles: Synthesis, Characterization, Properties, Applications, and Therapeutic Approaches. *Int J Mol Sci.* 2016 Sep 13;17(9):1534
18) More PR, Pandit S, Filippis A, Franci G, Mijakovic I, Galdiero M. Silver Nanoparticles: Bactericidal and Mechanistic Approach against Drug Resistant Pathogens. *Microorganisms*. 2023 Feb 1;11(2):369.
19) Gouyau J, Duval RE, Boudier A, Lamouroux E. Investigation of Nanoparticle Metallic Core Antibacterial Activity: Gold and Silver Nanoparticles against *Escherichia coli* and *Staphylococcus aureus. Int J Mol Sci.* 2021 Feb 14;22(4):1905.
20) Yuan YG, Peng QL, Gurunathan S. Effects of Silver Nanoparticles on Multiple Drug-Resistant Strains of Staphylococcus aureus and Pseudomonas aeruginosa from Mastitis-Infected Goats: An Alternative Approach for Antimicrobial Therapy. *Int J Mol Sci*. 2017 Mar 6;18(3):569.
21) Liao C, Li Y, Tjong SC. Bactericidal and Cytotoxic Properties of Silver Nanoparticles. *International Journal of Molecular Sciences*. 2019; 20(2):449.
22) Ghodake G, Kim M, Sung JS, Shinde S, Yang J, Hwang K, Kim DY. Extracellular Synthesis and Characterization of Silver Nanoparticles-Antibacterial Activity against Multidrug-Resistant Bacterial Strains. *Nanomaterials* (Basel). 2020 Feb 19;10(2):360.